SUPPLEMENTARY MATERIAL 2

Impact of the boundary conditions

In this supplementary material, we briefly present the calculation steps that allow incorporating the boundary conditions into the transfer matrix formalism, when considering a finite 1D-periodic medium with N unit cells immersed in water. The goal is here to demonstrate that the contribution of these boundary conditions on the ultrasound characteristics becomes insignificant when dealing with a sufficiently large number of unit cells.

In the manuscript, we showed that a wave propagating across a single unit cell (see Fig. 1) could be described using the transfer matrix given in Eq. (9). Based on this consideration,

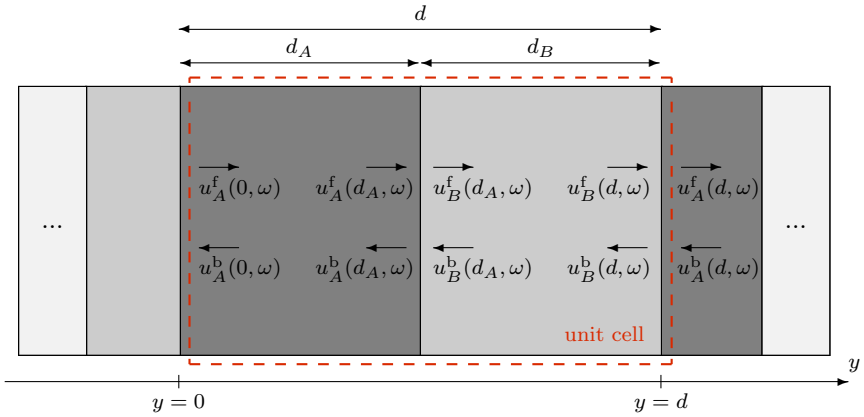

FIG. 1. Schematic representation of the transfer matrix formalism for a wave propagating across a single unit cell.

it is noteworthy that, when considering a medium made of N consecutive unit cells without external surrounding medium, there is no backward scattered wave causing a forward reflected wave in the very first layer, because there is no left boundary at $y = 0$. In addition, the right boundary at $y = Nd$ corresponds to an interface between the phases B and A, while in the immersed configuration, there should be an interface between the phase B and water, denoted by w. Thereby, the added interface at the left boundary $y = 0$ can be taken into account by adding a discontinuity matrix $\boldsymbol{D}_{wA}$ at the end of Eq. (10), while the modified impedance ratio at the right boundary can be accounted for by replacing the first discontinuity matrix $\boldsymbol{D}_{BA}$ by $\boldsymbol{D}_{Bw}$. Therefore, the total transfer matrix can now be expressed as

$$\boldsymbol{T}_N(\omega) = \boldsymbol{D}_{Bw}\boldsymbol{P}_B\boldsymbol{D}_{AB}\boldsymbol{P}_A\left(\boldsymbol{T}_{uc}\right)^{N-1}\boldsymbol{D}_{wA}\ . \tag{1}$$

Applying Sommerfeld radiation condition in water at the right boundary of the system, *i.e.*, $u_w^{\mathrm{f}}(Nd,\omega) = 0$, allows recovering the transfer function $H_N(\omega)$, which now relates the

transmitted wave $u_w^{\mathrm{f}}(Nd,\omega)$ to the incident wave $u_w^{\mathrm{f}}(0,\omega)$ in water as

$$H_N(\omega) = \frac{u_w^{\mathrm{f}}(Nd,\omega)}{u_w^{\mathrm{f}}(0,\omega)} = \frac{\det\left(\boldsymbol{T}_N(\omega)\right)}{T_{22}(\omega)} \ . \tag{2}$$

To calculate the apparent phase velocity $v_N(\omega)$ and attenuation $\alpha_N(\omega)$, the transfer function $H(\omega)$ needs to account for the added total transmission coefficient, which would otherwise be considered as attenuation. Thus, the transfer function can be modeled as

$$H_N(\omega) = T_{\mathrm{tot}_N}(\omega)\exp(-jk_N(\omega)y) \ , \tag{3}$$

with

$$T_{\mathrm{tot}_N}(\omega) = \frac{4Z_wZ_N(\omega)}{Z_w + Z_N(\omega))^2} \ , \tag{4}$$

where $Z_w = \rho_w c_w$ and $Z_N(\omega) = \rho_H v_N(\omega)$ are the acoustic impedances of water and that of the apparent homogeneous medium, respectively, with $\rho_H = (\rho_A d_A + \rho_B d_B)/d$ being its apparent homogeneous mass density. Thereby, Eqs. (12a)–(12b) of the manuscript now read as

$$v_N(\omega) = -\frac{\omega Nd}{\arg(H_N(\omega))} \ , \tag{5a}$$

$$\alpha_N(\omega) = \frac{1}{Nd}\ln\left(\left|\frac{T_{\mathrm{tot}_N}(\omega)}{H_N(\omega)}\right|\right) \ . \tag{5b}$$

Numerical examples

Figure 2 shows the apparent ultrasound characteristics (dashed red lines) for a water-immersed 1D-periodic medium, whose properties are those given in Fig. 2 of the manuscript (for water, we have taken $\rho_w = 998$ kg/m^3 and $v_w = 1500$ m/s). These are compared to the characteristics obtained without keeping the surronding medium into account (continuous black lines) for different numbers of unit cell repetitions N, while keeping the unit cell thickness d equal.

As can be observed, in the considered frequency range, the presence of water boundary conditions has a significant influence on the retrieved ultrasound characteristics for a low value of N. For an intermediate value of N, there are still slight differences, noticeable in particular in the low frequency range (oscillations due to Fabry-Perot interferences) and around the secondary bandgap. From the value $N = 8$, the impact of the surrounding medium becomes negligible, because the contribution of periodicity predominates.

Likewise, Figure 3 compares the modeling results obtained using the transfer matrix formalism with and without accounting for the presence of water, in the case of the three

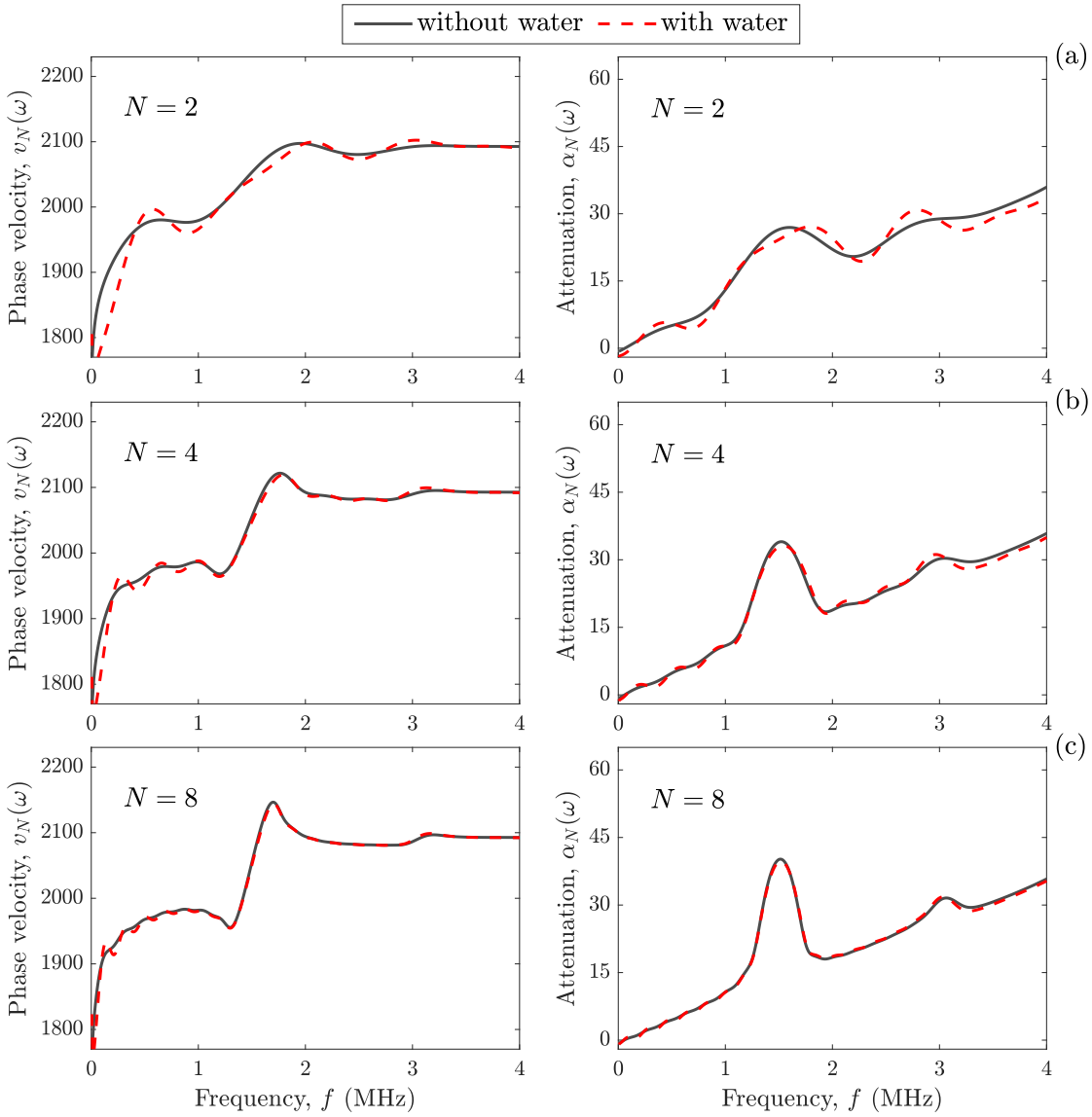

FIG. 2. Apparent ultrasound characteristics, *i.e.*, phase velocities $v_N(\omega)$ and attenuations $\alpha_N(\omega)$, obtained without surrounding water (continuous black lines) and with surrounding water (dashed red lines) for different numbers of unit cell repetitions N (with a fixed unit cell thickness $d = 677$ μm): (a) $N = 2$, (b) $N = 4$, and (c) $N = 8$. The constituent material properties used to feed the transfer matrix formalism are identical to those used in Fig. 2 of the manuscript.

investigated 1D-periodic samples (recall Fig. 9 in the manuscript). As can be observed, adding the two water-sample interfaces into the modeling has no significant impact on the apparent ultrasound characteristics, as the two curves (continuous black lines and dashed red lines) are almost superimposed, no matter the considered sample. The RMSE between the two curves is always less than 3 m/s and 1.2 dB/cm for the phase velocity and attenuation, respectively, and therefore lower than the expanded measurement uncertainties reported in the manuscript.

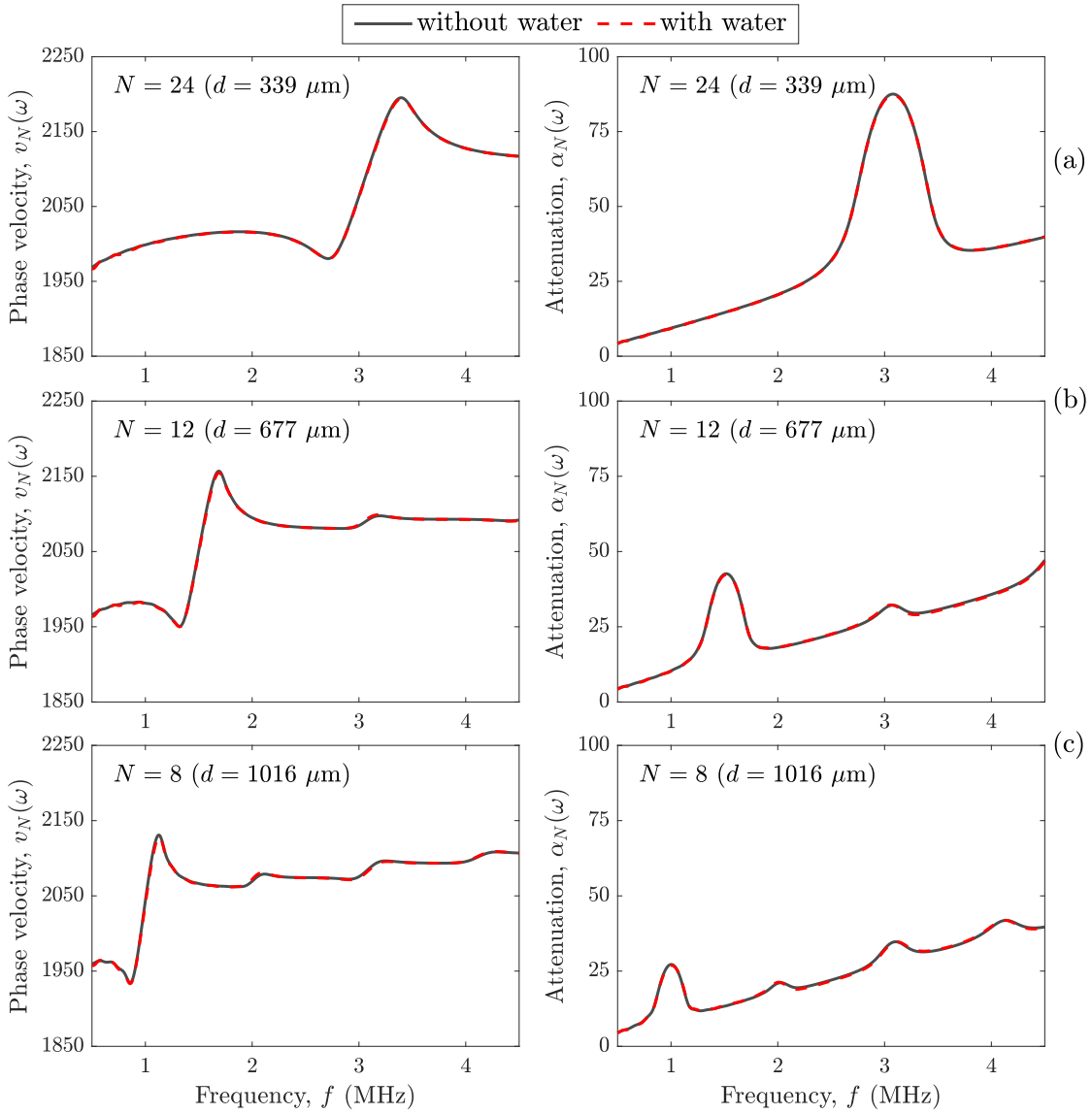

FIG. 3. Apparent ultrasound characteristics, *i.e.*, phase velocities $v_N(\omega)$ and attenuations $\alpha_N(\omega)$, obtained without surrounding water (continuous black lines) and with surrounding water (dashed red lines) for 1D-periodic AM samples with varying unit cell numbers and thicknesses: (a) $N = 24$ ($d = 339$ μm); (b) $N = 12$ ($d = 677$ μm), and (c) $N = 8$ ($d = 1016$ μm).

Overall, one can conclude that, from a sufficiently high number of unit cell repetitions ($N = 8$ in our case), it is not necessary to account for the surrounding medium in the transfer matrix formalism. This approach thereby provides us a modeling tool that can be concurrently compared to both the ultrasound measurements and the Bloch-Floquet analysis.